XLVI CILAMCE
VITÓRIA - ES - BRAZIL - 2025
XLVI IBERO-LATIN AMERICAN CONGRESS ON COMPUTATIONAL METHODS IN ENGENEERING

Numerical investigation of side wall influence in RHS column-I-beam welded connections

Diego Luiz Costa e Souza, Matheus Miranda de Oliveira, Arlene Maria Cunha Sarmanho, Vinícius Nicchio Alves

Dept. of Civil Engineering - DECIV, Federal University of Ouro Preto - UFOP
Ouro Preto, Minas Gerais - MG, Brazil
diego.luiz@aluno.ufop.edu.br, matheus.miranda@aluno.ufop.edu.br, arlene@ufop.edu.br, vinicius.alves@ufop.edu.br

Abstract. This study investigates the moment resistance and failure modes of welded connections between I-beams and rectangular hollow section (RHS) columns. The existing design codes and normative equations for estimating the moment resistance do not consider all geometric parameters that influence the behavior of the connections, such as the contribution of the side wall of the RHS. Using a validated finite element (FE) model, 315 uniplanar T-type welded connection models were evaluated, varying side wall thickness and height (t_0, h_0) of the RHS column, and beam dimensions (t_1, b_1, h_1). Two main failure modes were identified: frontal face plastification ($\beta \leq 0.85$) and side wall yielding ($\beta = 1.0$). Comparisons with EN 1993-1-8 and ISO 14346:2013 design codes revealed that current formulations underestimate moment resistance, especially at higher β values. Results show that increasing t_0 and β (beam-to-column width ratio) enhances the contribution of the side wall, improving connection resistance. A new equation is proposed to better account for side wall effects, offering more accurate resistance predictions, particularly for $\beta > 0.85$.

Keywords: Moment resistance, numerical analysis, rectangular hollow sections, side wall failure, tubular joints.

1 Introduction

Welded connections involving tubular profiles have drawn significant attention from researchers over the years. These types of profiles offer excellent mechanical and geometric properties, making them highly efficient for members subjected to compression, torsion, or combined loading. Their superior structural performance is mainly attributed to a larger radius of gyration, which increases their resistance to buckling. In contrast, I-sections exhibit superior flexural behavior, making them the preferred choice for beam elements, Wardenier [1].

Several studies - including those by Nizer et al. [2], Garifullin et al. [3], [4], [5], Park and Chao [6] Lópes-Colina et al. [7], [8], Lozano et al.[9], Serrano-López et al. [10], [11], Barros et al. [12], Gracia et .al [13] - have investigated the initial stiffness and the behavior of welded connections in RHS T-joints. These studies propose equations that represent the initial stiffness, mainly using the component method.

However, all of these studies focus on evaluating the initial stiffness rather than the moment resistance of the connection. Moreover, existing design standards ABNT NBR 16239:2013 [14], ISO 14346:2013[15] and EN 1993-1-8: 2021 [16] do not consider the influence of the column side walls in the connections. To address this gap, a parametric numerical study was conducted to assess how the side wall of the RHS column affects the moment resistance of the connection. Variations in the geometric properties of both beams and columns were analyzed, and von Mises stress distributions and displacement fields were evaluated. The numerical results were compared with the predictions provided by current design codes. Finally, a modification to the equation presented in ISO 14346 (2013) [15] was proposed considering the influence of this parameter, and the obtained results are more consistent.

2 Design Equations

The present study addresses this limitation by examining two governing failure mechanisms: (1) plastification of the column face, which normally governs when the beam-to-column width ratio ($\beta = b_1/b_0$) is within the range $0.4 \leq \beta \leq 0.85$, and (2) yielding of the column side wall, which becomes critical as β approaches unity.

The design equations in EN 1993-1-8 [16] and ISO 14346:2013 [15] estimate the moment resistance of the connection based on the governing failure mechanism. Both standards adopt the assumption that load transfer from the beam to the column occurs predominantly through the flanges. As a result, the equations provided by both codes incorporate analogous parameters and produce comparable strength predictions for the corresponding failure modes. The main distinction between the two is in the terminology and notation employed. Therefore, only the ISO 14346 equations are presented. Figure 1 illustrates the nomenclature of the geometric relationships adopted for these connections. Since the thickness of the flange (t_{f1}) is the same as the thickness of the beam web (t_{w1}) in all models, this parameter will be called simply t_1.

The axial resistance force for column frontal face failure (plastification) is determined by Eq. (1) and is valid for the range of $0.4 \leq \beta \leq 0.85$:

$$N_{1,Rd} = \sigma_{y0} {t_0}^2 \frac{2 + 2{,}8\beta}{\sqrt{1 - 0{,}9\beta}} Q_f \tag{1}$$

To determine the axial resistance force for column side wall failure, Eq. (2) can be used since $\beta \approx 1{,}0$:

$$N_{1,Rd} = \sigma_{y0} t_0 (2t_1 + 10t_0) Q_f \tag{2}$$

Q_f is a function that relates the normal stresses and the yield stress of the material (σ_{y0}), being taken equal to 1 for the cases studied because no axial force is imposed on the RHS column. For $0.85<\beta<1.0$, it is recommended to use interpolation between the axial resistance force obtained by Eq. (1) when $\beta = 0.85$ and by Eq. (2) when $\beta = 1.0$. Finally, the design moment resistance is obtained by multiplying the axial resistance force by the average height of the beam, as described in Eq. (3).

$$M_{1,Rd} = N_1 \, (h_1 - t_1) \tag{3}$$

The ultimate capacity of tubular joints be evaluated based on deformation limit criteria. In this study, this criterion proposed by Lu et al. [17], [18], was adopted to define the moment resistance in the numerical models. When the ratio between the numerical moment resistance at a deformation of $3\%b_0$ and that at deformation $1\%b_0$ is less than 1.5, the moment resistance is defined as the value corresponding to a deformation of $3\%b_0$, characterizing the ultimate limit state (ULS) of the connection. Conversely, if this ratio is greater than 1.5, the moment resistance should be limited to 1.5 times the value associated with a deformation of $1\%b_0$, which corresponds to the serviceability limit state (SLS). Furthermore, in cases where the maximum moment is reached before reaching the $3\%b_0$ deformation limit, this maximum moment should be adopted as the connection's moment resistance.

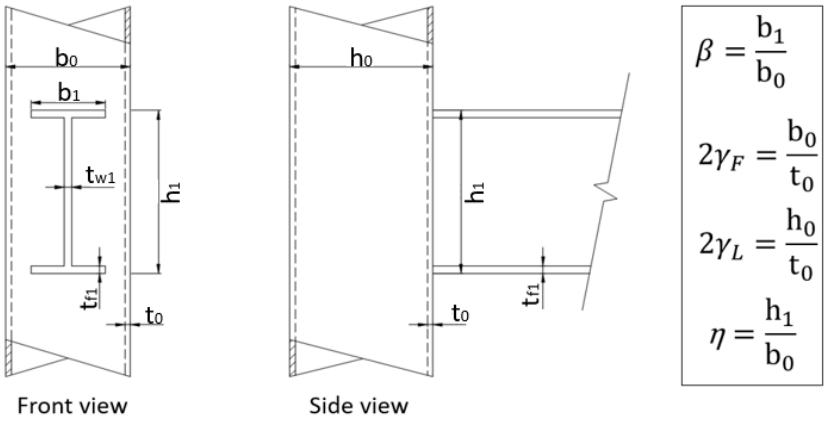


Figure 1.Geometric parameters

3 Numerical modelling and validation

The numerical model was developed using the finite element method, implemented in ANSYS 18. The connection geometry adopts a T-type configuration, comprising a rectangular hollow section (RHS) column and an I-section beam. To represent the corner curvature of the tubular profiles, a value equal to twice the wall thickness was adopted. Additionally, in accordance with the recommendations of the American Welding Society (AWS) [19] and ABNT NBR 16239 [14], the minimum weld size was defined as 1.5 times the lesser thickness between the beam and the column—corresponding, in all models, to the column wall thickness. The nominal material properties of the steels were incorporated into the finite element model using a bilinear isotropic hardening stress–strain relationship. The stress–strain curve included the yield strength (f_y), Young's modulus (E), and a tangent modulus (E_t) defined as E/100, as recommended by EN 1993-1-3 [20]. A Poisson's ratio of 0.3 was assumed for all elements.

The finite element SHELL281 was used to model the beams and columns due to demonstrated satisfactory performance in displacement and strain simulations in previous studies [10], [11], [12]. Welds were modeled using SOLID185 elements, as used in other studies [12], [21], [22]. Mapped mesh size of 10 mm was applied to ensure uniform element distribution and to minimize stress concentrations in the connection region. The characteristics of the numerical model are detailed in Figure 2.

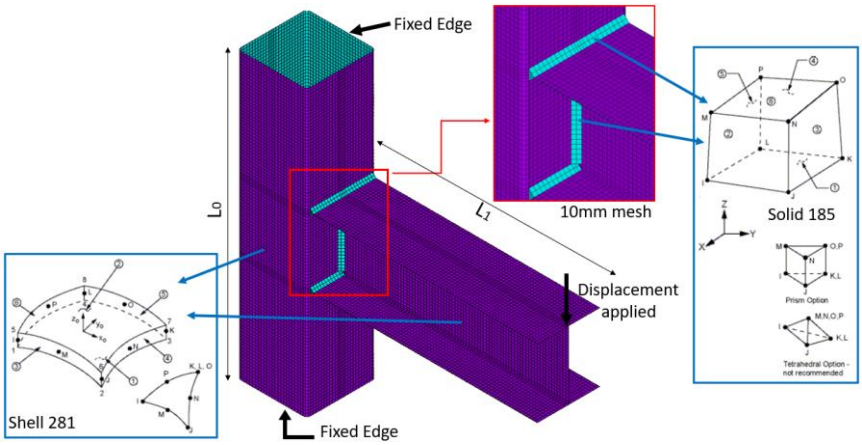


Figure 2. Finite element model

This numerical model was validated using experimental tests conducted by Barros [12], with β value of 0.5, which indicates the frontal face plastification as the predominant failure mode and by López-Colina et al. [7] and Serrano-López et al. [11], with β value of 1.0, where the side wall yielding is the failure mode, as shown in Costa e Souza [23] and in Fig. 3.

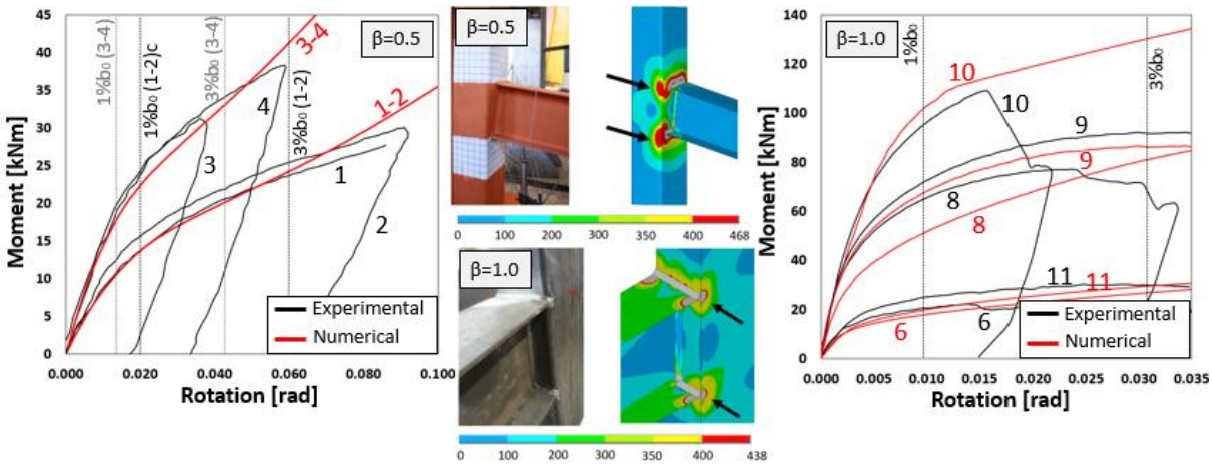


Figure 3. Validation of the numerical model

4 Parametric study

The parametric analysis was conducted to assess the impact of cross-sectional dimensions of columns and beams on the structural behavior of the connections. Specifically: a) For the columns, thickness values (t_0) of 4.0, 6.4, 7.1, 8.3 and 10 mm, and the side wall heights (h_0) of 150, 250 and 400 mm were adopted; b) For the beams, thicknesses (t_1) were taken as 1.5 times the columns thickness, widths (b_1) of 120, 200, 212.5, 225 and 250 mm, and Heights (h_1) of 150, 200, 250, 300 and 400 mm. The geometric configurations and relevant dimensionless ratios employed in the study are illustrated in Fig. 4. In order to more thoroughly examine the interpolation zone specified by ISO 14346 [15], additional variations in the beam height parameter (η) were introduced for models with β values of 1.0, 0.9, and 0.85. This combination of parameters resulted in a total of 315 numerical models.

For the RHS columns, the steel mechanical properties were defined with a yield strength (fy_0) of 345.0 MPa, an ultimate strength (fu_0) of 450.0 MPa and Young's modulus (E_0) of 205 GPa. To ensure that failure would occur in the column during the simulations, higher yield (fy_1) and ultimate (fu_1) strength values were adopted for the beams, as well as for the weld metal (f_w).

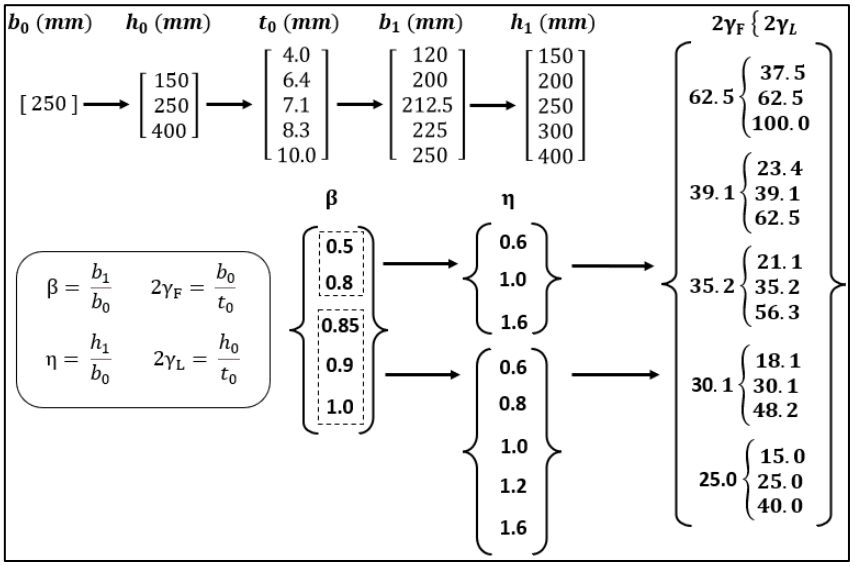


Figure 4. Variables of parametric study

5 Results and Discussion

5.1 Displacement and stress analysis

The maximum side wall displacements (d_{sw}) were mapped and compared to the maximum displacement of the front wall (d_{fw}), observed in the region compressed by the beam flange. A clear trend was identified: as the value of β increases, lateral displacements become more significant, indicating greater contribution from the side wall. When β=0.5, the displacement ratio (d_{sw}/d_{fw}) remains below 0.5, suggesting that the deformability of the model is predominantly governed by the front wall. When $0.9 \leq \beta < 1.0$ the displacement ratio generally exceeds 1, emphasizing the increased influence of the lateral wall under these conditions. A similar behavior is observed when β=1.0, where the failure mode is governed by the ultimate limit state (ULS) with a deformation criterion of $3\%b_0$. These results are illustrated in the moment x displacement curves in Fig. 5.

The frontal slenderness parameter ($2\gamma_F$) also has a significant influence on displacement levels: lower values of $2\gamma_F$ result in reduced displacements and leads to an increase in initial stiffness. The Von Mises stress distributions shown in Fig.6 further indicate that lower values of $2\gamma_F$, combined with higher β values, result in a greater contribution from the side wall. These results highlight a positive correlation can be identified between the contribution of the side wall.

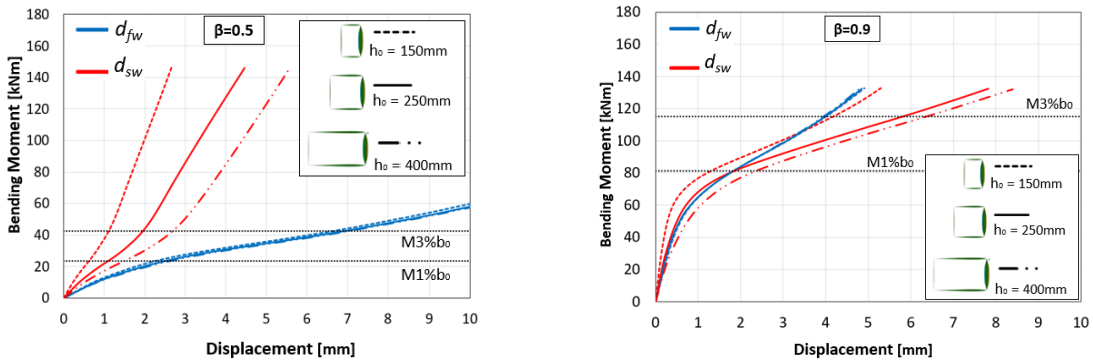


Figure 5. Bending Moment vs. Displacement curves – (a) β=0.5 and (b) β=0.9

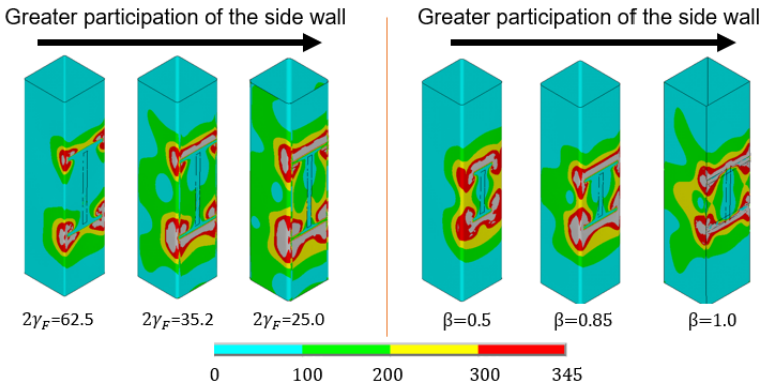


Figure 6. Von Misses Stress Distribution (MPa)

However, the accuracy of the analytical formulations is reduced precisely under these conditions. Moreover, variations in $2\gamma_L$ are sufficient to produce noticeable differences in side wall displacements and in the corresponding moment resistances. Therefore, the limited accuracy of the normative equation under these conditions may be attributed to the unaccounted influence of the side wall, which should be considered.

5.2 New equation proposal

A new analytical equation is proposed for β=1.0, as this case showed the largest discrepancy between analytical and numerical results. It also involves significant side wall contribution and a defined failure mode, justifying specific attention. Improving the formulation for β =1.0 also benefits the interpolation range 0.85<β<1.0.

The proposed equation incorporates the effective area of the RHS column wall contributing to moment resistance, based on stress distribution analysis. Three key regions were identified—horizontal front wall, vertical front wall, and side wall, as illustrated in Fig.7. The parameters $2\gamma_F$, $2\gamma_L$, and η were included into this new formulation described in the Eq. 4. Their coefficients were iteratively calibrated according to the observed yielding behavior in each region.

$$N_T = \sigma_{y0} t_0 \left[(4t_1 + 20t_0) \frac{{2\gamma_L}^{0,01}}{{2\gamma_F}^{0,35}} + (2t_1 + 10t_0) K_\gamma + (2t_1 \eta^{-0,3}) {2\gamma_F}^{-0,2} \right] \tag{4}$$

where:

$$\begin{cases} 2\gamma_F > 40 \rightarrow K_\gamma = {2\gamma_F}^{-0,4} \\ 2\gamma_F \leq 40 \rightarrow K_\gamma = {2\gamma_F}^{-0,35} \end{cases} \tag{5}$$

It is important to note that the proposed Eq. (4) is valid for the parameter ranges $25.0 \leq 2\gamma_F \leq 62.5$ with $15 \leq 2\gamma_L \leq 100$ and $0.6 \leq \eta \leq 1.6$, for a yield stress of f_{y0} = 345 MPa.

Figure 8 presents a comparison between the normative equation (Eq. (2)) and the proposed formulation (Eq. (4)) against the numerical results. The proposed equation demonstrated satisfactory accuracy across the 87 models with β=1.0 analyzed in this study. As a result, it also improved the predictions for an additional set of 75 models with β=0.9, which fall within the interpolation range 0.85<β<1.0.

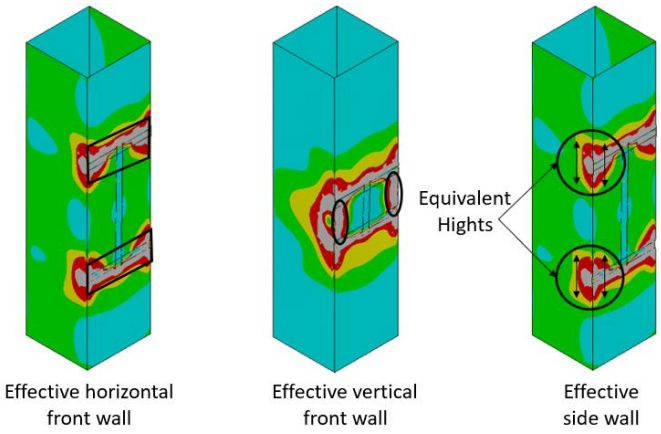


Figure 7. RHS column effective walls

Table 1 compares the mean and coefficient of variation (CoV) values for the analytical-to-numerical moment resistance ratio evaluating both equations. These results demonstrate the effectiveness of the proposed equation in predicting the connection's moment resistance ratio under the studied conditions.

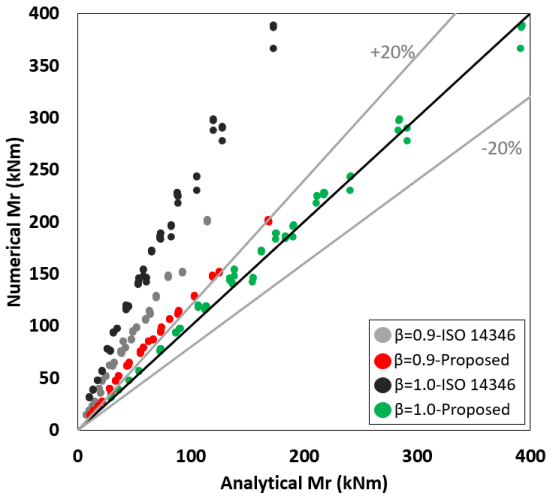


Figure 8. Moment resistance: Numerical vs. Analytical

Table 1. $M_{r,AN}/M_{r,NUM}$ - Mean and CoV - ISO 14346 vs. Proposed

β	ISO 14346		Proposed	
	Mean	CoV	Mean	CoV
1.0	0.383	0.085	0.959	0.041
0.9	0.527	0.074	0.762	0.054

6 Conclusions

Side wall participation is most prominent when low $2\gamma_F$ values are combined with high β, with lateral slenderness ($2\gamma_L$) further influencing behavior in these configurations. Existing design equations showed limited accuracy due to their conservative nature and neglect of side wall effects. In this context, a modified equation based on ISO 14346 was proposed for β=1.0, incorporating key parameters (β, η, $2\gamma_F$, and $2\gamma_L$). This formulation significantly improved prediction accuracy, increasing the mean analytical-to-numerical resistance ratio from 0.383 to 0.959 and reducing the coefficient of variation from 0.085 to 0.041. Similar improvements were observed for β=0.9. However, the proposed equation is valid only for the parameter ranges $25.0 \leq 2\gamma_F \leq 62.5$ with $15 \leq 2\gamma_L \leq 100$ and $0.6 \leq \eta \leq 1.6$, with a yield stress of f_{y0} = 345 MPa. In this context, future work should extend the parameter range to include η>1.6, $2\gamma_F$<25, alternative steel grades, and values of β≤0.85 to further refine the model and broaden its applicability.

Acknowledgements. The authors thank CAPES, CNPq and UFOP for suporting this research.

Authorship statement. The authors hereby confirm that they are the sole liable persons responsible for the authorship of this work, and that all material that has been herein included as part of the present paper is either the property (and authorship) of the authors, or has the permission of the owners to be included here.

References

[1] Wardenier J., "Hollow Section Joints", Phd Thesis, Thechische Universiteit Delft, Delft, The Netherlands, 1982.

[2] A. Nizer *et al.*, "Experimental and numerical assessment of RHS T-joints subjected to brace and chord axial forces", *Steel Construction*, vol. 9, nº 4, p. 315–322, 2016, doi: 10.1002/stco.201610036.

[3] M. Garifullin, S. Pajunen, K. Mela, e M. Heinisuo, "Finite element model for rectangular hollow section T joints", *Rakenteiden Mekaniikka*, vol. 51, nº 3, p. 15–40, dez. 2018, doi: 10.23998/rm.70439.

[4] J. Havula, M. Garifullin, M. Heinisuo, K. Mela, e S. Pajunen, "Moment-rotation behavior of welded tubular high strength steel T joint", *Eng Struct*, vol. 172, p. 523–537, out. 2018, doi: 10.1016/J.ENGSTRUCT.2018.06.029.

[5] M. Garifullin, M. Bronzova, S. Pajunen, K. Mela, e M. Heinisuo, "Initial axial stiffness of welded RHS T joints", *J Constr Steel Res*, vol. 153, p. 459–472, fev. 2019, doi: 10.1016/J.JCSR.2018.10.025.

[6] K. S. Park e S. H. Chao, "Strength of transverse plate-to-rectangular HSS connection under single-concentrated compression", *J Constr Steel Res*, vol. 199, dez. 2022, doi: 10.1016/j.jcsr.2022.107606.

[7] C. López-Colina, M. A. Serrano, M. Lozano, F. L. Gayarre, J. M. Suárez, e T. Wilkinson, "Characterization of the main component of equal width welded I-beam-to-RHS-column connections", *Steel and Composite Structures*, vol. 32, nº 3, p. 337–346, ago. 2019, doi: 10.12989/scs.2019.32.3.337.

[8] C. López-Colina, M. A. Serrano, M. Lozano, F. L. Gayarre, e J. M. Suárez, "Stiffness of equal width welded I-beam to RHS column connection", 2021, doi: 10.1002/cepa.

[9] M. Lozano, M. A. Serrano-López, C. López-Colina, e Y. C. Wang, "Contribuitions of welded web to rotational stiffness and bending moment capacity of 'I beam-RHS column' joints", em *Tubular Structures XVI: Proceedings of the 16th International Symposium for Tubular Structures (ISTS)*, Heidarpour e Zhao, Orgs., Melbourne: Taylor & Francis Group, 2018, p. 4–6.

[10] M. A. Serrano-López, C. López-Colina, J. González, e F. López-Gayarre, "A simplified FE simulation of welded I beam-to-RHS column joints", *International Journal of Steel Structures*, vol. 16, nº 4, p. 1095–1105, dez. 2016, doi: 10.1007/s13296-016-0028-5.

[11] M. A. Serrano-López, C. López-Colina, Y. C. Wang, M. Lozano, e F. L. Gayarre, "Comparative behaviour of 'I beam- RHS column' joints with and without web weld", *J Constr Steel Res*, vol. 159, p. 330–340, ago. 2019, doi: 10.1016/j.jcsr.2019.05.002.

[12] H. T. G. de Barros, M. M. de Oliveira, A. M. C. Sarmanho, e V. N. Alves, "Stiffness assessment of welded I-beam to RHS column connections", *Eng Struct*, vol. 267, set. 2022, doi: 10.1016/j.engstruct.2022.114661.

[13] J. Gracia, M. Lozano, C. López-Colina, e M. A. Serrano-López, "Characterisation of new components of unequal-width welded I-beam–RHS-column connections", *Journal of Building Engineering*, vol. 86, jun. 2024, doi: 10.1016/j.jobe.2024.108626.

[14] ABNT NBR 16239, *Projetos e estruturas de aço e mistas de aço e concreto de edificações com perfis tubulares*, 1.ed. Rio de Janeiro: Associação Brasileira de Normas Técnicas, 2013. [Online]. Disponível em: www.abnt.org.br

[15] ISO 14346, *Static design procedure for welded hollow-section joints - Recommendations*, 1.ed. Switzerland: International Organization for Standardization, 2013.

[16] prEN 1993-1-8, *Eurocode 3: Design of steel structures. Draft Part 1-8: Design of joints*. Brussels, Belgium: CEN (European Commitee of Standardization), 2021.

[17] L. H. Lu, "The static strength of I-beam to rectangular hollow section column connections", PhD Thesis, Delft University, Netherlands, 1997.

[18] L. H. Lu, G. D. Winkel, Y. Yu, e J. Wardenier, "Deformation Limit for the ultimate strength of hollow sections joints", em *Proceedings 6th International Symposium on Tubular Structures*, B. R. Tubular Structures VI, Org., Melbourne, Australia: The Netherlands, 1994, p. 341–347.

[19] American Welding Society, *AWS D1.1/D1.1 M. Structural welding code-steel*. Miami: American Welding Society, 2010.

[20] EN 1993-1-3, *Eurocode 3: Design of steel structures - Part 1-3: General rules - Supplementary rules for cold-formed members and sheeting*. Brussels, Belgium: CEN (European Commitee of Standardization), 2006.

[21] V. B. P. de Souza, A. T. da Silva, M. C. Rodrigues, e L. R. O. de Lima, "Experimental and numerical assessment of reinforced SHS T-joints with doubler plate", *Structures*, vol. 70, dez. 2024, doi: 10.1016/j.istruc.2024.107759.

[22] M. Pandey, K. F. Chung, e B. Young, "Numerical investigation and design of fully chord supported tubular T-joints", *Eng Struct*, vol. 239, jul. 2021, doi: 10.1016/j.engstruct.2021.112063.

[23] D. L. Costa e Souza, M. M. de Oliveira, A. M. C. Sarmanho, e V. N. Alves, "Influence of the side wall of RHS columns on the behavior of welded connections with I-beam sections", *Journal of Building Engineering*, vol. 111, p. 113189, out. 2025, doi: 10.1016/j.jobe.2025.113189.